Biochemical Pharmacology, Vol. 38, No. 14, pp. 2329–2338, 1989.
Printed in Great Britain.

0006-2952/89 $3.00 + 0.00

AVERMECTIN BINDING IN *CAENORHABDITIS ELEGANS*

A TWO-STATE MODEL FOR THE AVERMECTIN BINDING SITE

JAMES M. SCHAEFFER* and HERBERT W. HAINES
Merck Sharp & Dohme Research Laboratories, Rahway, NJ 07065, U.S.A

(*Received* 18 *March* 1988; *accepted* 13 *December* 1988)

Abstract—Specific binding sites for ivermectin (IVM; 22,23-dihydroavermectin-B_1) were identified and characterized in a crude membrane fraction prepared from the nematode, *Caenorhabditis elegans (C. elegans)*. Specific [^{3}H]IVM binding was saturable with an apparent dissociation constant, K_d, of 0.26 nM and a receptor concentration of 3.53 pmol/mg protein. [^{3}H]IVM binding in *C. elegans* was linear with tissue protein concentration, and optimal binding occurred within a pH range of 7.3 to 7.6. Kinetic analysis of the binding showed that the reaction proceeded by a two-step mechanism. Initially, a rapidly reversible complex was formed and, after additional incubation, this complex was transformed to a much more slowly reversible complex. Stereospecificity of [^{3}H]IVM binding to *C. elegans* membranes was demonstrated by competition with a series of avermectin derivatives. The *in vivo* effects of IVM and its derivatives on *C. elegans* motility were concentration dependent and correlated well with their relative binding affinities. Several putative neurotransmitters including γ-aminobutyric acid (GABA), carbamyl choline, taurine, glutamate and dopamine were tested and found to have no effect on IVM binding. Specific IVM binding sites were also identified in rat brain; however, the affinity was approximately 100-fold lower than that observed in *C. elegans* and stereospecificity studies demonstrated structural differences in the two binding sites. These results are the first direct demonstration of a specific IVM binding site in nematodes and thus are important in furthering our understanding of its mode of action.

Avermectins (AVM†) are a family of macrocyclic lactones isolated from *Streptomyces avermitilis* [1, 2] which have potent anthelmintic [3, 4] and insecticidal [5] activities. Structurally, AVMs possess a 16-membered lactone ring with a spiroacetal system (C-17 to C-25) consisting of two six-membered rings and an α-L-oleandrosyl-α-L-oleandrosyloxy disaccharide substituent at the C-13 position [6, 7]. The naturally occurring AVMs can be separated into four major components (A_{1a}, A_{2a}, B_{1a}, and B_{2a}),, of which the B series are generally more biologically active. A synthetic derivative of B_1, 22,23-dihydroavermectin (B_1 ivermectin), has been developed for veterinary and medical use [8, 9].

The mode of action of the avermectins remains unclear. Electrophysiological experiments using crustacea demonstrated that high concentrations of AVM (1.2 to 12 μM) irreversibly block inhibitory postsynaptic potentials as a result of increased chloride ion conductance [10, 11]. The AVM stimulated increase in membrane conductance could be inhibited by bicuculline and picrotoxin (GABA antagonists), suggesting that AVM acts at the level of the GABA-gated chloride ion channel. In addition, AVM blocks the signal transmission from ventral interneurons to excitatory motorneurons in the parasitic nematode *Ascaris*, and this blockade can also be reversed by picrotoxin [12]. Duce and Scott [13] have investigated the actions of IVM on the extensor tibiae muscle of the locust *Schistocerca gregaria*. This muscle has fibers which receive inhibitory innervation and are known to be GABA sensitive, and other fibers which receive excitatory innervation and are GABA insensitive. Low concentrations of AVM (0.009 to 9.0 nM) reversibly increase the chloride permeability of the GABA-sensitive fibers. Higher doses of AVM (0.012 to 1.2 μM) produce an irreversible increase in chloride permeability in both the GABA-sensitive and -insensitive muscle fibers. These results suggest the existence of multiple sites of action for IVM, one of which is independent of the GABA receptor–Cl ion channel complex.

Several laboratories have reported data suggesting that avermectins modulate specific binding of GABA [14, 15] and benzodiazepines [15–18] in rat brain membrane preparations. To further explore the interaction of AVM with specific binding sites, [^{3}H]IVM has been used for ligand binding studies. Specific high-affinity binding sites have been identified in rat and dog brain preparations [19, 20]; however, no studies have described the presence of specific AVM binding sites in tissues from AVM-sensitive target organisms. In this report, we describe

* Correspondence: Dr James M. Schaeffer, Merck Sharp & Dohme Research Laboratories, R80T-132, P.O. Box 2000, Rahway, NJ 07065.

† Abbreviations: AVM, Avermectin (2aE,4E,5′S,-6S,6′R,7S,8E,11R,15S,17aR,20R,20aR,20bS)6′[(R)R-*sec*-butyl]-7-[[2,6,dideoxy-4-*O*-(2,6-dideoxy-3-*O*-methyl)-α-Larabino-hexopyranosyl-3-*O*-methyl-α-L-arabino-hexopyranosyl]oxy]-5′,6,6′,7,10,11,14,15,17a,20,20a,20b-dodecahydro-20,20b-dihydroxy-5′,6,8,19-tetramethyl-spiro-[11,15-methano-2*H*,13*H*,17*H*-furo-4,3,2,-pq][2,6]benzodioxyacyclo-octadecin-13,3′[2*H*]pyran]-17-one); HEPES, 4-(2-hydroxyethyl)-1 piperazineethane sulfonic acid; and GABA, γ-aminobutyric acid.

the binding of [^{3}H]IVM to membranes isolated from *Caenorhabditis elegans*, a free living nematode which is extremely sensitive to AVM [12, 21]. The characteristics of [^{3}H]IVM binding to *C. elegans* membranes are distinct from binding in mammalian systems and may enable us to further understand the mechanism by which this class of anthelmintic compounds works.

MATERIALS AND METHODS

Chemicals. The avermectins were supplied by Drs H. Mrozik and M. Fisher, Merck Sharp & Dohme Research Laboratories (Rahway, NJ). [^{3}H]Ivermectin was labeled at the 22,23-position by catalytic hydrogenation with tritium gas to a specific activity of 51.9 Ci/mmol. Purity of [^{3}H]ivermectin was confirmed using thin-layer chromatography on silica gel 60-F 254 (E.M. Laboratories, Inc.). The plate was developed with chloroform–ethyl acetate–methanol–methylene chloride (9:9:1:2). The R_f value was 0.51, and the [^{3}H]IVM was found to be greater than 95% pure. The other compounds were purchased from commercial sources.

Nematode cultures. C. elegans, N_2 strain, was obtained from Dr T. Mellin, Merck Sharp & Dohme Research Laboratories (Rahway, NJ). The nematodes were cultivated on NG agar plates covered with a lawn of *Escherichia coli*, as previously described [22]. Worms (all stages) were washed off the plates with 50 mM HEPES buffer, pH 7.4, homogenized in a Braun Cell Homogenizer (using 0.45 mm glass beads) for 15 sec, and then centrifuged for 5 min at 1,000 *g*. The pellet (P_1) was discarded, and the supernatant fraction (S_1) was centrifuged for 20 min at 28,000 *g*. The resulting pellet (P_2) was resuspended in HEPES buffer to approximately 12.5 μg protein/ml and used for the membrane binding assays.

Rat brain tissue preparation. Male rats (Sprague–Dawley, 250–300 g) were decapitated, and the cerebral cortices were quickly removed and homogenized in 10 vol. of 50 mM HEPES buffer, pH 7.4, at 4° with a glass–glass homogenizer. The homogenate was centrifuged for 5 min at 1,000 *g*, and the resulting supernatant fraction was centrifuged for 20 min at 28,000 *g*. The P_2 pellet was resuspended in HEPES buffer (1 mg protein/ml) and used immediately to measure [^{3}H]IVM binding.

Binding assays. The membrane preparations (1.0 ml) were incubated with [^{3}H]IVM at 22° for 45 min in the presence (nonspecific binding) or absence (total binding) of a 500-fold molar excess of unlabeled ivermectin in glass tubes (13 × 100 mm). The incubation was terminated by rapid filtration over Whatman GF/B filters (pretreated with 0.15% polyethylimine and 0.5% Triton X-100 in order to minimize nonspecific binding) and rinsed with 15 ml (3 × 5 ml) of ice-cold HEPES buffer containing 0.25% Triton X-100. The filters were placed into glass vials containing 10 ml Aquasol II (New England Nuclear, Boston, MA), and the radioactivity was determined by liquid scintillation spectrometry at 62% efficiency. Specific binding was calculated by subtracting nonspecific from total binding.

Caenorhabditis elegans *motility assays.* Worms were rinsed off the agar plates with Krebs' bicarbonate buffer (124 mM NaCl, 5 mM KCl, 26 mM $NaHCO_3$, 1.2 mM KH_2PO_4 and 1.3 mM $MgSO_4$; pH 7.4, at 22°), washed two times by centrifugation at 500 *g* for 2 min, and then resuspended into Krebs' buffer. Aliquots (50 μl) containing approximately 100 worms each were then placed into 13 × 100 mm glass test tubes. The avermectins were dissolved in dimethyl sulfoxide and added to the test tubes containing the worms in a final volume of 500 μl with 1% dimethyl sulfoxide. After 16 hr of incubation at 22°, the motility was determined by examination with a low power dissecting microscope. Greater than 90% of the worms continued to swim vigorously in the control tube. The percentage of immotile worms was then determined at several concentrations of each avermectin derivative.

Protein concentrations were determined using the dye staining technique of Bradford [23], with bovine serum albumin as the standard.

RESULTS

Optimal conditions for [^{3}H]ivermectin binding. To determine the optimal tissue preparation for *C. elegans*, [^{3}H]IVM binding was measured in whole homogenate and various subcellular fractions. As shown in Table 1, the specific activity of [^{3}H]IVM binding sites was enriched approximately 4-fold in the P_2 pellet (3.0 pmol/mg protein) as compared to the whole homogenate (0.70 pmol/mg protein). In addition, approximately 73% of the total binding activity was recovered in the P_2 fraction; consequently, this preparation was used in subsequent binding experiments.

Specific [^{3}H]IVM binding increased linearly as a function of tissue protein concentration between 0.007 and 0.32 mg protein/ml. The optimum pH for binding was fairly broad, with greater than 75%

Table 1. Subcellular localization of [^{3}H]ivermectin binding sites

Fraction	Total protein (mg)	Total binding (pmol)	Specific activity (pmol/mg)
Homogenate	8.32	5.85	0.70
S_1 Supernatant	6.02	5.43	0.90
P_1 Pellet	2.64	0.56	0.21
S_2 Supernatant	4.16	2.17	0.52
P_2 Pellet	1.44	4.30	3.00

The tissue preparation and binding assays were performed as described in the text, in the presence of 2.2 nM [^{3}H]IVM.

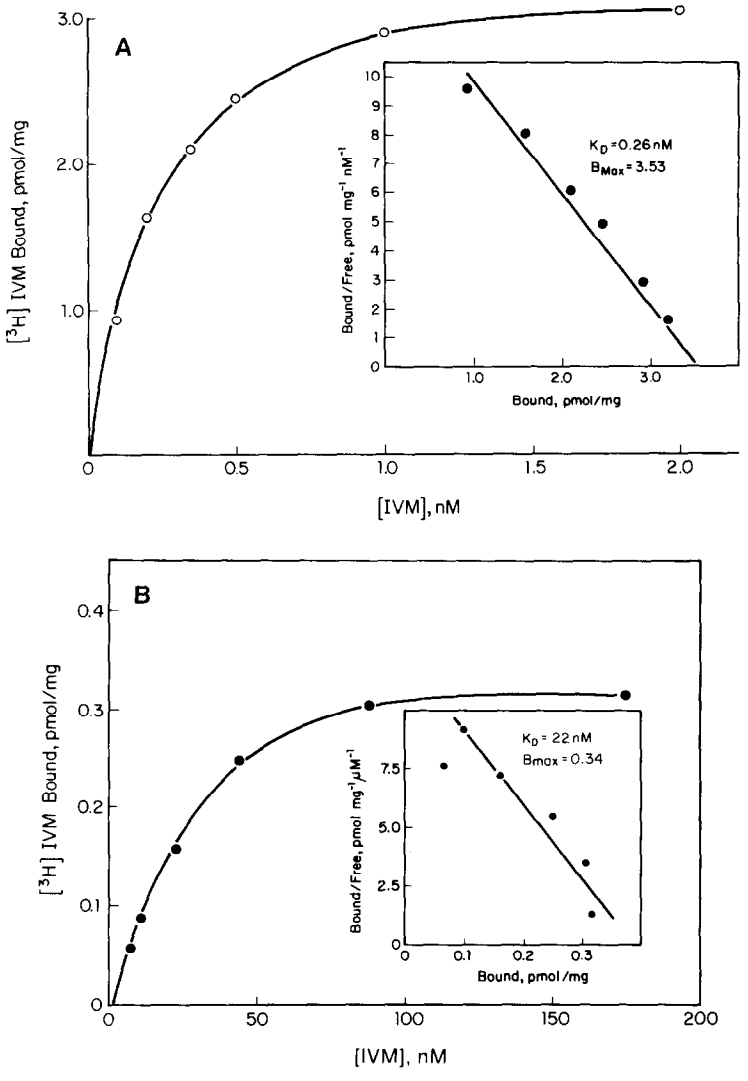

Fig. 1. (A) Equilibrium binding of [^{3}H]IVM to *C. elegans* membranes. Increasing concentrations of [^{3}H]IVM were incubated with *C. elegans* membranes, and specific binding was determined as described in the text. Each point is the average of four determinations. Replicate experiments gave similar results. A Scatchard analysis (inset) of the saturation data is shown. (B) Similar experiments were performed using rat cerebral cortex membranes.

maximal binding between 7.1 and 7.6. Incubation in buffer with higher or lower pH values resulted in sharply decreased [^{3}H]IVM binding (data not shown).

Equilibrium binding parameters. C. elegans membranes were incubated for 45 min at 22° in the presence of increasing concentrations of [^{3}H]IVM (0.055 to 2.2 nM) with (nonspecific) or without (total binding) a 500-fold molar excess of unlabeled IVM. Specific [^{3}H]IVM binding to membrane fractions was saturable with increasing concentrations of [^{3}H]IVM (Fig. 1A). The Scatchard analysis (Fig. 1A, inset) of these data yielded a straight line, consistent with the existence of a single class of [^{3}H]IVM binding sites. The binding site had a high affinity (K_d = 0.26 nM) and low capacity (3.53 pmol/mg protein). Nonspecific binding increased linearly and was approximately 22% of total binding at 2.2 nM [^{3}H]IVM.

Specific IVM binding was also examined using membrane fractions from rat cerebral cortex. As shown in Fig. 1B, [^{3}H]IVM bound in a saturable manner with an apparent dissociation constant (K_d) of 22 nM and a B_{max} of 0.34 pmol/mg protein.

Binding kinetics. The rate of binding of various concentrations of [^{3}H]IVM at 22° is illustrated in Fig. 2. At each concentration, the binding reaction proceeded without a lag and reached 50% saturation at approximately 2–10 min; a constant amount of ligand binding was achieved between 10 and 30 min. The amount of [^{3}H]IVM bound at steady state increased with the concentration of ligand. If the binding reaction is a reversible bimolecular reaction, the integrated rate equation is given by $\ln[B_{eq}/(B_{eq} - B_t)] = (k_{+1}[\text{IVM}] + k_{-1})t$ where B_{eq} and B_t are the amount of IVM bound at equilibrium (60 min) and at time t; k_{+1} is the second order rate

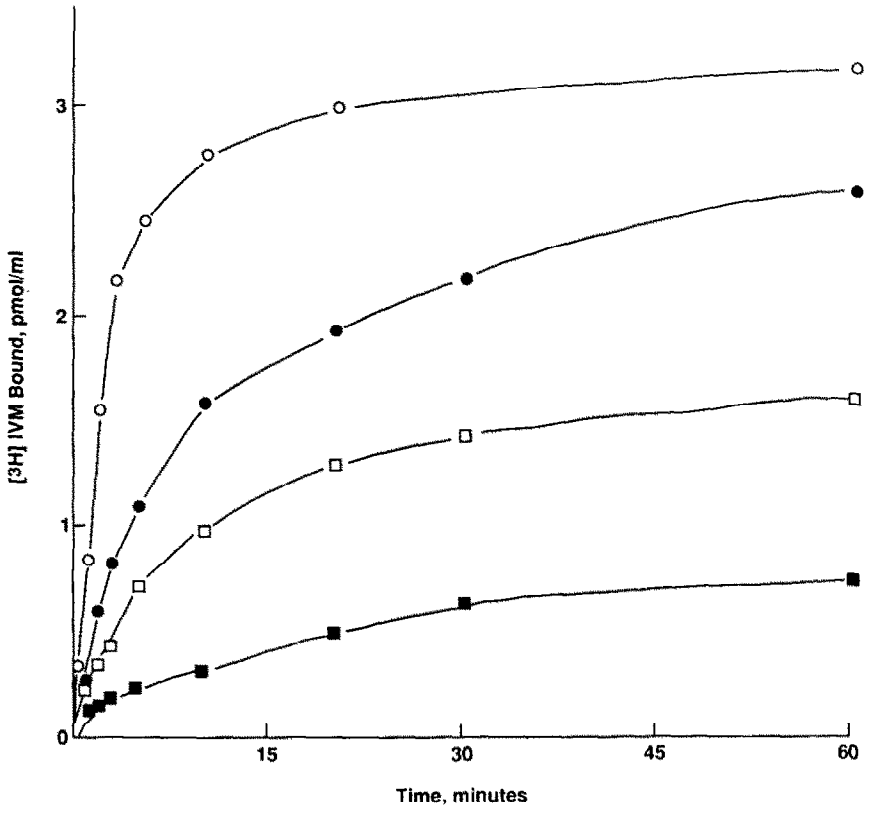

Fig. 2. Rate of association of specific [^{3}H]IVM binding to *C. elegans* membranes. Specific binding was measured as a function of time with various concentrations of [^{3}H]IVM [0.22 nM (■), 0.55 nM (□), 1.1 nM (●) and 2.2 nM (○) at 22°, as described in the text. Each point is the average of at least four determinations.

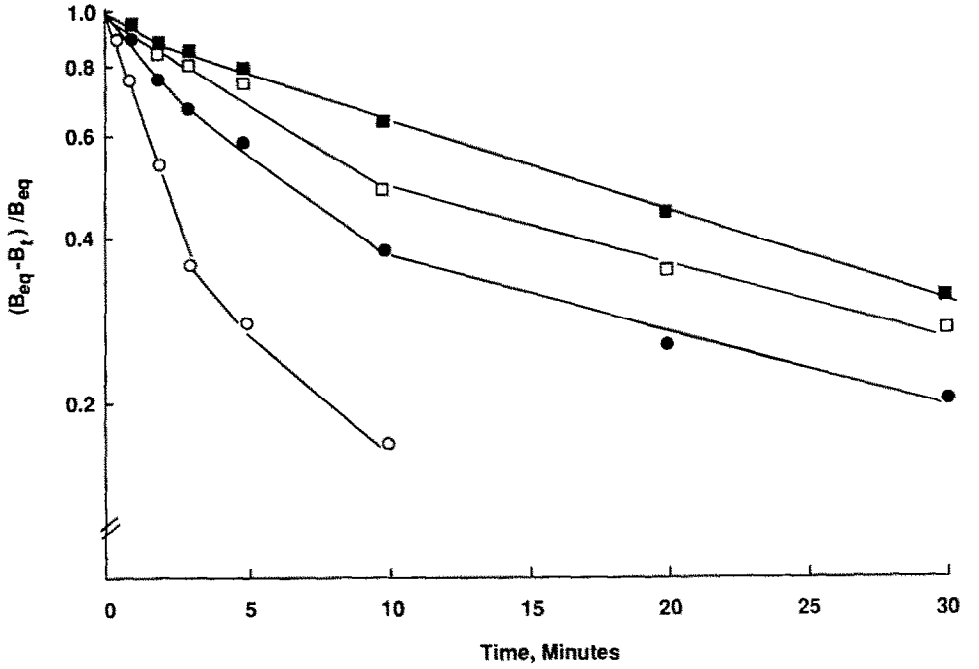

Fig. 3. Initial rate of [^{3}H]IVM binding to *C. elegans* membranes at different IVM concentrations. *C. elegans* membranes were incubated with 0.22 (■), 0.55 (□), 1.1 (●) and 2.2 (○) nM [^{3}H]IVM for the indicated times, and specifically bound IVM was determined as described in Materials and Methods. The data are plotted according to the equation described in the text. Each point is the average of at least four determinations.

constant and k_{-1} is the rate constant for the dissociation reaction. Since IVM was in large excess, it remained constant during the reaction. Data from an experiment in which initial rates of binding were determined for four concentrations of IVM are plotted according to this equation in Fig. 3. The data did not define a straight line, suggesting that the reaction is not a simple bimolecular reaction. These data could result from concurrent reactions of IVM with two distinct binding sites (R′ and R″) having different kinetic properties:

$$\begin{aligned} \text{IVM} + \text{R}' &\rightleftharpoons \text{IVM}\cdot\text{R}' \\ \text{IVM} + \text{R}'' &\rightleftharpoons \text{IVM}\cdot\text{R}'' \end{aligned} \quad (1)$$

or a two-step sequential reaction of a rapid formation of a reversible, low-affinity ligand–receptor complex followed by a higher affinity, more stable complex:

$$\text{IVM} + \text{R} \underset{k_{-1}}{\overset{k_1}{\rightleftharpoons}} \text{IVM}\cdot\text{R} \underset{k_{-2}}{\overset{k_2}{\rightleftharpoons}} \text{IVM}\cdot\text{R}^*. \quad (2)$$

The ordinate intercept, obtained by extrapolating the linear portion of the time curves in Fig. 3 to $t = 0$, provides the fraction of total sites which reacted slowly. The data indicate that the intercept changes as the initial IVM concentration is increased. This is consistent with a fast binding component converting to a slower, higher affinity site and excludes the possibility that we are observing two independent, parallel reactions in which the percentage of fast-reacting binding sites should be constant as a function of the IVM concentration.

The sequential reaction described in equation 2 predicts the existence of a low-affinity complex initially present in high concentrations and decreasing as a function of time. To test this hypothesis, the rate of dissociation of IVM was determined after the binding site was exposed to 2.2 nM [^{3}H]IVM for either 2 or 45 min (Fig. 4). In each case, the dissociation was biphasic. After the 2-min incubation, approximately 60% of the bound IVM dissociated rapidly ($T_{\frac{1}{2}} = 2$ min), whereas after 45 min only 15–18% of the bound IVM dissociated rapidly. Similar results were obtained whether the dissociation rate was measured after simple dilution of the [^{3}H]IVM, dilution into excess unlabeled IVM (as in Fig. 4), or dilution into excess AVM B_{1a} 4″-*O*-phosphate. These results provide evidence that initially most of the IVM is bound in a rapidly reversible complex and, during subsequent incubation, this complex is transformed to a more slowly reversible complex.

To further substantiate this sequential mechanism, we measured the concentration of rapidly reversible and slowly reversible complexes as a function of reaction time (Fig. 5). Bound [^{3}H]IVM not dissociating during a 15-min incubation in the presence of excess IVM was defined as slowly reversible. These experiments show that a rapidly reversible complex formed quickly, reached a maximum concentration by 3–5 min, and then diminished. The slowly reversible complex appeared more slowly and continued to increase until greater than 90% of the total bound IVM appeared slowly reversible by 40 min. Control experiments showed that the reversible binding component was stable under the incubation conditions and, therefore, that the loss of reversibly bound [^{3}H]IVM cannot be due to denaturation of a specific class of reversible binding

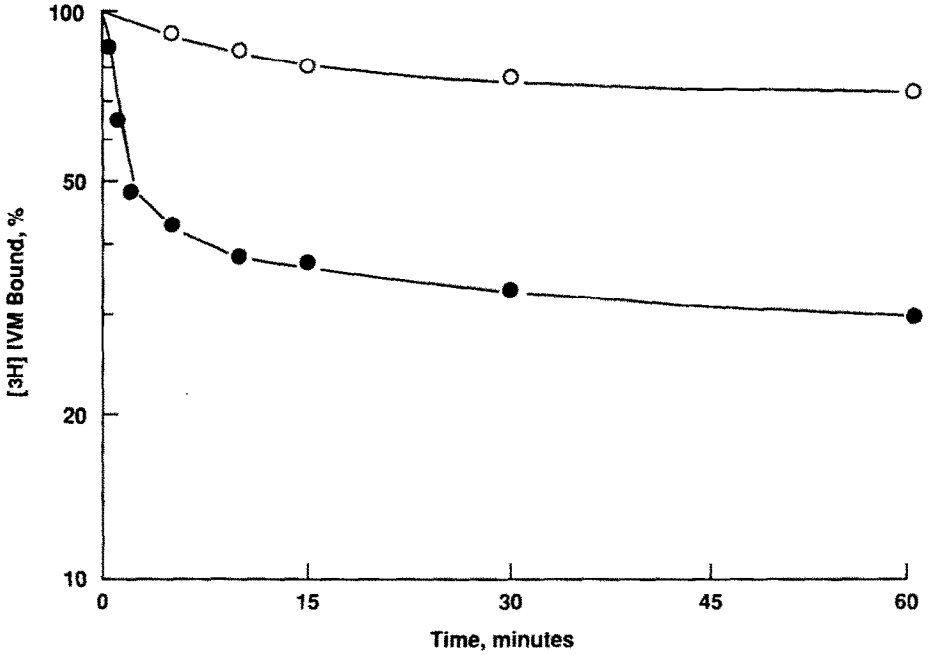

Fig. 4. Rate of dissociation of [^{3}H]IVM. *C. elegans* membranes were incubated with 2.2 nM [^{3}H]IVM for 2 (●) or 45 (○) min. Unlabeled IVM (1.0 μM) was then added, and the incubation continued for the indicated times. Specifically bound [^{3}H]IVM was quantitated as described in the text. At zero time, 0.18 pmol of [^{3}H]IVM was bound in the samples incubated for 2 min and 0.54 pmol of [^{3}H]IVM in those incubated for 45 min. Each point is the average of at least four determinations.

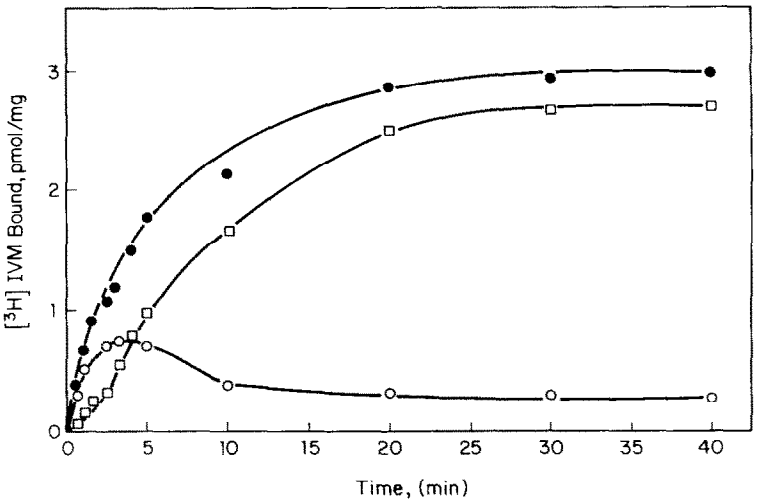

Fig. 5. Rate of formation of reversible and irreversible [^{3}H]IVM binding site complexes. *C. elegans* membranes were incubated with 2.2 nM [^{3}H]IVM at 22° for the times indicated. Two aliquots were taken at the indicated time, and total [^{3}H]IVM bound (●) was measured using one aliquot as described in Materials and Methods. Irreversibly bound [^{3}H]IVM (□) was measured by diluting the second aliquot into excess unlabeled IVM (1.0 μM), incubating for 15 min at 22° to allow reversibly bound [^{3}H]IVM to dissociate, and finally measuring bound [^{3}H]IVM. Reversibly bound [^{3}H]IVM (○) was calculated by subtracting the irreversibly bound [^{3}H]IVM from the total bound [^{3}H]IVM. Each point is the average of at least four determinations.

sites. These results strongly suggest a precursor/product relationship between the reversible and irreversible complexes and support a sequential mechanism as shown in equation 2 above.

The dissociation rate constant, k_{-1} (from equation 2), can be estimated from the initial slope of the data in Fig. 4 (after a 45-min incubation with 2.2 nM [^{2}H]IVM) to be 0.14 min^{-1}. The value of ([IVM]$k_1 + k_{-1}$) for the reversible phase of the reaction can be estimated from the initial slope of the data in Fig. 3. for 2.2 nM IVM where most of the binding observed was reversible. In four experiments, the average value of ([IVM]$k_1 + k_{-1}$) was 0.38. This corresponds to $k_1 = 0.12 \times 10^9$ M^{-1} min^{-1}. There is some uncertainty in this estimate since, in plotting the data, the value of B_{eq} actually represents the sum of both the reversible and irreversible reaction rather than B_{eq} for the reversible phase alone. This value is, therefore, an underestimate of k_1; however, the error should not exceed 26%. The value of K_d for the reversible reaction (k_{-1}/k_1) to give 50% saturation of the sites after a 45-min incubation (0.26 nM, Fig. 1A) was substantially less than the binding constant for the reversible phase of the reaction. This reflects the fact that the slowly reversible phase of the binding reaction resulted in a complex of higher affinity. Our present data do not allow us to calculate rate constants or binding constant for the slowly reversible phase of the reaction.

Kinetic studies of [^{3}H]IVM binding to rat brain membranes were also performed. In contrast to the *C. elegans* system, the IVM–receptor interaction in rat brain membranes is a single-step reaction. Rat brain membranes were incubated in the presence of 110 nM [^{3}H]IVM at 22° for varying lengths of time, and specific binding was determined. As shown in Fig. 6, the rate of association was rapid, reaching 50% maximum binding within 5 min, and plateauing between 30 and 60 min. The rate of association was estimated to be 0.065 nM^{-1} min^{-1}. The rate of dissociation (Fig. 6, inset) was determined by incubating

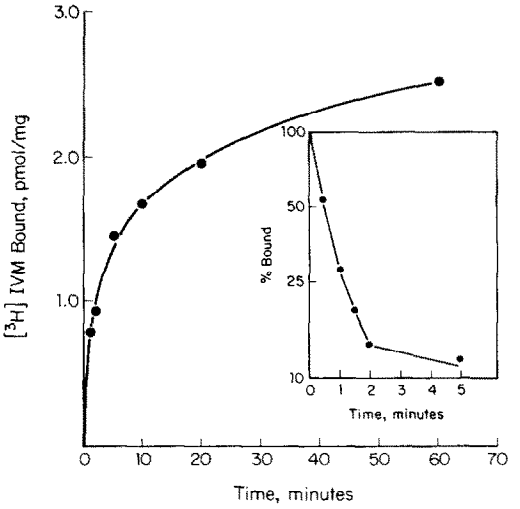

Fig. 6. Rate of association of specific [^{3}H]IVM binding to rat cerebral cortex membranes. Specific binding was measured as a function of time with a saturating concentration of [^{3}H]IVM (110 nM) at 22°. The k_1 value was derived from the initial slope. Each point represents the average of four determinations: the SE was less than 10%. The rate of dissociation (inset) was determined by adding 11 μM AVM B_{1a} 4″-*O*-phosphate at 60 min and measuring displacement of [^{3}H]IVM. A logarithmic analysis of the data is shown in the inset.

the membranes for 60 min in the presence of 110 nM [^{3}H]IVM. A 100-fold molar excess of AVM B_{1a} 4″-*O*-phosphate was then added to the incubation medium, and the rate of decline of specifically bound [^{3}H]IVM was measured as a function of time. AVM B_{1a} 4″-*O*-phosphate was used due to its relatively high solubility in aqueous solutions. The half-life of the [^{3}H]IVM–binding site complex was approximately 0.5 min, and the rate constant for dissociation was 1.35 min^{-1}. Using the equation $K_d = k_{-1}/k_1$, we calculated a K_d value of 21 nM for IVM binding to rat brain membranes. This was 100-fold lower affinity than with *C. elegans* membranes and demonstrates a major difference between the invertebrate and mammalian binding site for IVM.

Stereospecificity of [^{3}H]IVM binding. To assess the specificity of [^{3}H]IVM binding, the abilities of various avermectin derivatives to compete with [^{3}H]IVM for specific binding sites were determined (Fig. 7). Invermectin, AVM B_{2a} and AVM B_{1a} 4″-*O*-phosphate were the most potent inhibitors of specific [^{3}H]IVM binding [inhibition constant (K_i) values between 0.1 and 0.3 nM, see Fig. 7]. 22,23-Dihydro-AVM B_{1a} aglycone, 22,23-dihydro-AVM B_1 monosaccharide, AVM B_1 monosaccharide, 2-dehydro-4-hydro-α-2,3-AVM B_1 and AVM B_{1a}-5-ketone were less potent inhibitors and had K_i values between 0.7 and 1.1 nM. 2,3,8,9,10,11,22,23-octahydro-AVM B_{1a} had no significant effect on specific [^{3}H]IVM binding at concentrations up to 100 nM. The potencies of these AVM derivatives were determined

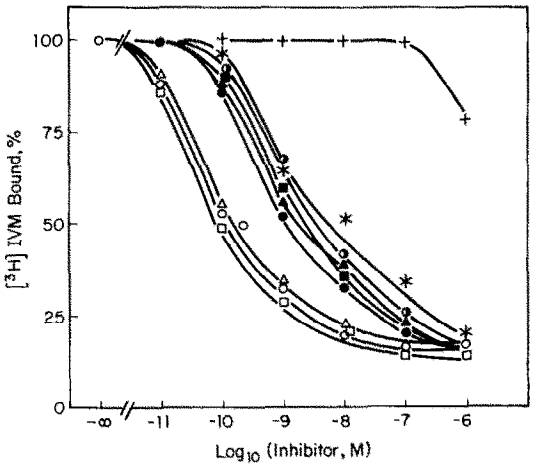

Fig. 7. Inhibition of specific [^{3}H]IVM binding to *C. elegans* membranes by AVM analogs. *C. elegans* membranes were incubated with 0.22 nM [^{3}H]IVM in the presence or absence of various AVM derivatives. K_i values were determined using the formula: $K_i = IC_{50}/(1 + c/K_d)$, where the IC_{50} is the concentration of the drug required to inhibit 50% of the specific binding (determined by log probit plots), and c is the concentration of [^{3}H]IVM. The compounds examined were IVM (□), AVM B_{2a} (○), AVM B_{1a} 4″-*O*-phosphate (△), 22,23-dihydro-AVM B_{1a} aglycone (●), 22,23-dihydro-AVM B_1 monosaccharide (■), AVM B_1 monosaccharide (▲), 2-dehydro-4-hydro-α-2,3-AVM B_1 (◑), AVM B_{1a}-5-ketone (*) and 2,3,8,9,10,11,22,23-octahydro-AVM B_{1a} (+). Each point is the average of at least four determinations.

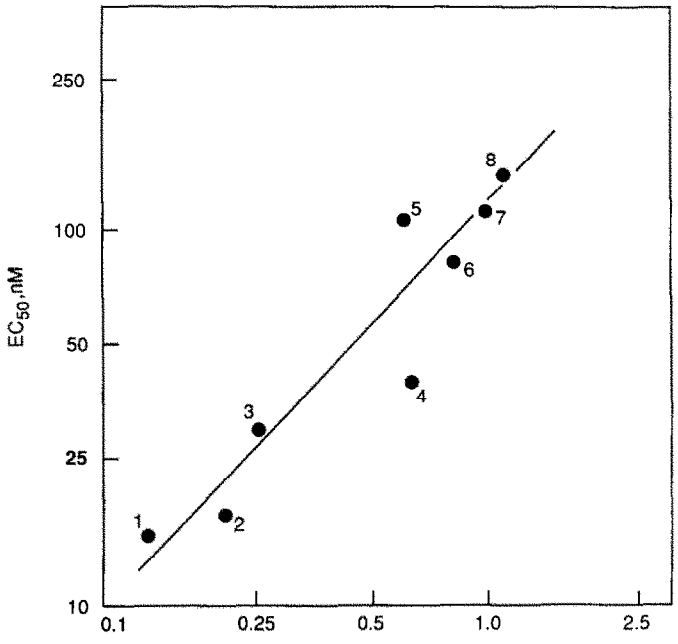

Fig. 8. Correlation between binding affinities of AVM analogs and their biological potencies on *C. elegans* motility *in vivo*. Inhibition constants (K_i) are from Fig. 7. The motility of *C. elegans* was determined as described in the text. The EC_{50} is the concentration of AVM needed to produce immotility in 50% of the worms. The results are the mean values from two to ten experiments, each one having at least three determinations (SE less than 15%). A correlation coefficient (r) of 0.975 was calculated by linear regression analysis. For the log-log plot, $r = 0.923$. The compounds tested were: (1) IVM; (2) AVM B_{2a}; (3) AVM B_{1a} 4″-*O*-phosphate; (4) 22,23-dihydro-AVM B_{1a} aglycone; (5) 22,23-dihydro-AVM B_1 monosaccharide; (6) AVM B_1 monosaccharide; (7) 2-dehydro-4-hydro-α-2,3-AVM B_1 and (8) AVM B_{1a}-5-ketone. 2,3,8,9,10,11,22,23-Octahydro-AVM B_{1a} is not shown since this compound had no quantifiable K_i value.

in vivo using a *C. elegans* motility assay and, as shown in Fig. 8, we observed a close correlation between bioactivity and the relative binding affinities of the AVM analogs.

The affinities of several hundred avermectin analogs for the IVM binding site have been determined in both *C. elegans* and rat brain membrane preparations. The purpose of these studies was to identify analogs which differentially bind to *C. elegans* membranes and not rat brain membranes in order to develop more efficacious and safer avermectins. As shown in Table 2, the 13-deoxy-avermectins have been identified as analogs with relatively high affinity for the *C. elegans* site and a markedly reduced affinity for the rat brain binding site. These data further demonstrate the structural differences between IVM binding sites in *C. elegans* and rat brain.

GABA effect of [^{3}H]IVM binding. Electrophysiological [10, 11, 24] and biochemical [19, 20] studies have suggested that GABA interacts at the IVM binding site. Consequently, we examined the effects of various GABA agonists and antagonists on specific IVM binding. None of the compounds tested [GABA, muscimol, (+)-bicuculline, picrotoxin and diazepam] had any effect on [^{3}H]IVM binding at concentrations up to 10 μM (data not shown). In addition, several putative neurotransmitters (dopamine, taurine, carbamyl choline and norepinephine) were also tested and had no effect on specific [^{3}H]IVM binding at concentrations up to 1 mM.

DISCUSSION

We have demonstrated the presence of specific IVM binding sites in the nematode *Caenorhabditis elegans*. *C. elegans* was chosen to be used in this study for several reasons: it is a simple, well-studied organism; the adult has 811 somatic cells, 302 of which are neurons; the neuronal interconnections have been anatomically defined [25, 26] and many putative neurotransmitters have been identified [27–29]; and *C. elegans* is extremely sensitive to IVM *in vivo* [12, 21]. The interaction of IVM with its binding site occurred via a two-step mechanism which was markedly different from the interaction of IVM with its binding site in rat brain tissue. The dissociation constant and receptor concentration of IVM binding sites in *C. elegans* were calculated to be 0.26 nM and 3.53 pmol/mg protein respectively (Fig. 1A). The specificity of IVM binding to its receptor was demonstrated by the competition of binding by several avermectin analogs (Fig. 7). The relative potencies of the avermectin analogs as inhibitors of receptor binding paralleled their effects on *C. elegans* motility (Fig. 8). The close correlation between biological effect and relative binding affinities of a series of AVM analogs supports the physiological significance of the IVM binding site. The apparent difference in potency of ivermectin in the binding assay and motility assay may be due to availability of the drug to the site of action. Under *in vivo* conditions, the percentage of immotile worms increased as a function of time for up to 120 hr. Specific binding of [^{3}H]IVM to rat brain membranes was approximately 100-fold lower affinity, suggesting a profound difference between the IVM binding site in *C. elegans* and rat brain. This difference has been further characterized by comparison of the K_i values for hundreds of avermectin analogs determined with *C. elegans* and rat brain membrane preparations. As illustrated in Table 2, the sugar moiety was crucial for the ligand–receptor interaction in rat brain tissue, whereas with *C. elegans* membranes, IVM and its aglycone analogs had relatively similar K_i values (0.2 to 6.4 nM). These data suggest that in *C. elegans* the interaction of IVM with its binding site does not require the sugar moiety.

Table 2. Inhibition of [^{3}H]IVM binding by 13-substituted 22,23-dihydro-avermectin B_{1a} aglycones

C-13-Substituent	K_i (nM) *C. elegans*	K_i (nM) Rat brain
IVM	0.2	21
H_2	0.9	123
α-OH	6.4	>3000
keto	0.6	239
β-Cl	1.0	1275
β-F	0.3	290
β-I	2.4	>3000

K_i values for each compound were determined as described in Materials and Methods.

Electrophysiological and biochemical studies have demonstrated that IVM alters chloride permeability of the cell membranes and results in an increased flux of chloride ions in crustacea [10, 11], insects [13, 24], nematodes [30], and rat synaptosomal preparations [31, 32]. GABA-sensitive inhibitory neurons also have increased chloride permeability in response to GABA, and the IVM-mediated increase in membrane permeability to chloride ions appears to be antagonized by GABA antagonists [10, 11, 24, 31, 32]. Consequently, it was suggested that IVM acts at the GABA binding complex or, conversely, that GABA interacts with the IVM binding site. The effects of GABA and GABA analogs on specific [^{3}H]IVM binding to rat brain membranes are somewhat controversial. Drexler and Sieghart [20] report that IVM binding is allosterically inhibited by GABA agonists, whereas Pong and Wang [14] report no effect of GABA antagonists on [^{3}H]AVM binding. Using membranes prepared from *C. elegans*, we observed no effect of GABA, picrotoxin, or bicuculline on IVM binding. Furthermore, no diazepam binding site was present in the *C. elegans* membrane preparation (data not shown).

Kinetic analysis of the IVM–receptor complex present in *C. elegans* revealed a time-dependent change in the rate of dissociation (Fig. 4). Initially, the rate of dissociation was rapid and then decreased as the time of association was increased. These results demonstrate that the IVM–receptor interaction conforms to a two-step mechanism: formation of a rapidly reversible complex followed by conversion to a much more slowly reversible form as described in equation 2. The existence of a two-step sequential mechanism of binding is supported by the observation that the rapidly reversible IVM–binding site complex reached a maximum concentration

within 5 min and then diminished, whereas the percentage of slowly reversible complexes increased as a function of time (Fig. 5). Similar two-step mechanisms of association have been described for insulin [33], α-bungarotoxin [34] and quinuclidinylbenzoate [35] binding. Kinetic studies of IVM receptors in rat brain were conducted, and only a single binding component was observed.

The differences in rates of dissociation of IVM from the receptor in *C. elegans* and rat brain are consistent with K_d values determined by binding studies conducted under equilibrium conditions (Fig. 1A and B). Our results clearly demonstrate major differences between the IVM binding site in a nematode and mammalian brain tissue preparations. As shown in Table 2, the removal of the disaccharide from IVM did not alter markedly its binding characteristics to *C. elegans*, whereas these compounds had almost no affinity for the rat brain binding site. Since *C. elegans* is sensitive to IVM, it is a logical source of tissue to study the mode of action of IVM. The physiological importance of the conversion to a slowly dissociating IVM binding site in *C. elegans* is not known although it may lead to our better understanding of the differential effects of AVMs in parasite and host systems.

Acknowledgements—The authors wish to thank Drs M. J. Turner, M. H. Fisher and H. Mrozik for their interest in this project and Mrs J. Wood and Ms K. Rosa for their assistance in the preparation of this manuscript.

REFERENCES

1. Miller TW, Chaiet L, Cole DJ, Flor JE, Goegelman RT, Gullo VP, Joshua H, Kempf AJ, Krellwitz WR, Monaghan RL, Ormond RE, Wilson DE, Albers-Schonberg G and Putter I, Avermectins, a new family of potent anthelmintic agents: isolation and chromatographic properties. *Antimicrob Agents Chemother* **15**: 368–371, 1979.
2. Burgh RW, Miller BM, Baker EE, Birnbaum J, Currie JA, Hartman R, Kong V-L, Monaghan RL, Olson G, Putter I, Tunac JP, Wallick H. Stapley EO, Oiwa R and Omura S, Avermectins, a new family of potent anthelmintic agents: producing organism and fermentation. *Antimicrob Agents Chemother* **15**: 361–367, 1979.
3. Egerton JR, Ostlind DA, Blair LS, Eary CH, Suhayda D, Cifelli S, Riek RF and Campbell WC, Avermectins, a new family of potent anthelmintic agents: efficacy of the B_{1a} component. *Antimicrob Agents Chemother* **15**: 372–378, 1979.
4. Putter I, MacConnell JG, Preiser FA, Haidri AA, Ristich SS and Dybas RA, Avermectins: novel insecticides, ascarids and nematicides from a soil microorganism. *Experientia* **37**: 963–964, 1981.
5. Ostlind DA, Cifelli S and Lang R, Insecticidal activity of the antiparasitic avermectins. *Vet Rec* **105**: 168, 1979.
6. Albers-Schonberg G, Arison BH, Chabala JC, Douglas AW, Eskola P, Fisher MH, Lusi A, Mrozik H, Smith TL and Tolman RL, Structure determination of avermectins. *J Am Chem Soc* **103**: 4221–4224, 1981.
7. Springer JP, Arison BH, Hirshfield JM and Hoogsteen K, The absolute stereochemistry and conformation of avermectin B_{2a} aglycone and avermectin B_{1a}. *J Am Chem Soc* **103**: 4216–4221, 1981.
8. Fisher MH and Mrozik H, The avermectin family of macrolide-like antibiotics. In: *Macrolide Antibiotics* (Ed. Omura S), pp. 553–606. Academic Press, New York, 1984.
9. Cupp EW, Bernardo MJ, Kiszewski AE, Collins RC, Taylor HR, Aziz MA and Greene BM, The effects of ivermectin on transmission of *Oncocerca volvulus*. *Science* **231**: 740–742, 1986.
10. Fritz LC, Wang CC and Gorio A, Avermectin B_{1a} irreversibly blocks postsynaptic potentials at the lobster neuromuscular junction by reducing muscle membrane resistance. *Proc Natl Acad Sci USA* **76**: 2062–2066, 1979.
11. Mellin TN, Busch RD and Wang CC, Postsynaptic inhibition of invertebrate neuromuscular transmission by avermectin B_{1a}. *Neuropharmacology* **22**: 89–96, 1979.
12. Kass IS, Wang CC, Walrond JP and Stretton AOW, Avermectin B_{1a}, a paralyzing anthelmintic that affects interneurons and inhibitory motoneurons in *Ascaris*. *Proc Natl Acad Sci USA* **77**: 6211–6215, 1980.
13. Duce IR and Scott RH, Actions of dihydroavermectin B_{1a} on insect muscle. *Br J Pharmacol* **85**: 395–401, 1985.
14. Pong SS and Wang CC, Avermectin B_{1a} modulation of 4-aminobutyric acid receptors in rat brain membranes. *J Neurochem* **38**: 375–379, 1982.
15. Olsen RW and Snowman AM, Avermectin B_{1a} modulation of gamma-aminobutyric acid/benzodiazepine receptor binding in mammalian brain. *J Neurochem* **44**: 1074–1082, 1985.
16. Drexler G and Sieghart W, Evidence for association of a high affinity avermectin binding site with the benzodiazepine receptor. *Eur J Pharmacol* **101**: 201–207, 1984.
17. Williams M and Risley EA, Avermectin interactions with benzodiazepine receptors in rat cortex and cerebellum *in vitro*. *J Neurochem* **42**: 745–753, 1984.
18. Pong SS, DeHaven R and Wang CC, Stimulation of benzodiazepine binding to rat brain membranes and solubilized receptor complex by avermectin B_{1a} and 4-aminobutyric acid. *Biochim Biophys Acta* **646**: 143–150, 1981.
19. Pong SS and Wang CC, The specificity of high affinity binding of avermectin B_{1a} to mammalian brain. *Neuropharmacology* **19**: 311–317, 1980.
20. Drexler G and Sieghart W, Properties of a high affinity binding site for [^{3}H]avermectin B_{1a}. *Eur J Pharmacol* **99**: 269–277, 1984.
21. Simpkin KG and Coles GC, The use of *Caenorhabditis elegans* for anthelmintic screening. *J Chem Technol Biotechnol* **31**: 66–69, 1981.
22. Brenner S, The genetics of *Caenorhabditis elegans*. *Genetics* **77**: 71–94, 1974.
23. Bradford MM, A rapid and sensitive method for the quantitation of microgram quantities of protein utilizing the principle of protein dye binding. *Anal Biochem* **72**: 248–258, 1976.
24. Tanaka D and Matsumura F, Action of avermectin B_{1a} on the leg muscles and the nervous system of the American cockroach. *Pestic Biochem Physiol* **24**: 124–135, 1985.
25. Ward S, Thomson N, White JG and Brenner S, Electron microscopical reconstruction of the anterior sensory anatomy of the nematode *Caenorhabditis elegans*. *J Comp Neurol* **610**: 313–338, 1975.
26. Ware RW, Clark C, Crossland K and Russell RL, The nerve ring of the nematode *Caenorhabditis elegans*. *J Comp Neurol* **162**: 71–110, 1975.
27. Sulston JE, Dew M and Brenner S, Dopaminergic neurons in the nematode *Caenorhabditis elegans*. *J Comp Neurol* **163**: 215–226, 1975.
28. Johnson C, Druckett J, Culotti J, Herman R, Neneely P and Russell R, An acetylcholinesterase-deficient mutant of the nematode *Caenorhabditis elegans*. *Genetics* **97**: 261–279, 1981.

29. Horvitz RH, Chalfie M, Trent C, Sulston JE and Evans PD, Serotonin and octopamine in the nematode *Caenorhabditis elegans*. *Science* **216**: 1012–1014, 1982.
30. Kass IS, Larsen S, Wang CC and Stretton AOW, The effects of avermectin and drugs related to acetylcholine and 4-aminobutyric acid on neurotransmission in *Ascaris suum*. *Mol Biochem Parasitol* **13**: 213–225, 1982.
31. Matsumoto K, Yamazaki J, Minako K and Fukuda H, The actions of ivermectin on cultured chick spinal cord neurons. *Neurosci Lett* **69**: 279–284, 1986.
32. Abalis IM, Eldefrawi AT and Eldefrawi ME, Actions of avermectin B_{1a} on the gamma-aminobutyric acid, receptor and chloride channels in rat brain. *J Biochem Toxicol* **1**: 69–82, 1986.
33. Corin RE and Donner DB, Insulin receptors convert to a higher affinity state subsequent to hormone binding. *J Biol Chem* **257**: 104–110, 1982.
34. Hess GP, Bulger JE, Fu JL, Hindey EF and Silberstein RJ, Allosteric interactions of the membrane-bound acetylcholine receptor; kinetic studies with alpha-bungarotoxin. *Biochem Biophys Res Commun* **64**: 1018–1027, 1976.
35. Galper JB, Klein W and Catterall WA, Muscarinic acetylcholine receptors in developing chick heart. *J Biol Chem* **252**: 8692–8699, 1977.